

SATURATION EFFECT ON PHOTOIONIZATION-DRIVEN BROAD ABSORPTION LINE VARIABILITY

WEI-JIAN LU (陆伟坚)¹ AND YING-RU LIN (林樱如)²

School of Information Engineering, Baise University, Baise 533000, China

¹E-mail: william_lo@qq.com (W-J L)²E-mail: yingru_lin@qq.com (Y-R L)

ABSTRACT

We study the saturation effect on broad absorption line (BAL) variability through a variation phenomenon, which shows significant variation in Si IV BAL but no or only small change in C IV BAL (hereafter Phenomenon I). First, we explore a typical case showing Phenomenon I, quasar SDSS J153715.74+582933.9 (hereafter J1537+5829). We identify four narrow absorption line (NAL) systems within its Si IV BAL and two additional NAL systems within its C IV BAL, and confirm their coordinated weakening. Combining with the obvious strengthening of the ionizing continuum, we attribute the BAL variability in J1537+5829 to the ionization changes caused by the continuum variations. Secondly, a statistical study based on multi-observed quasars from SDSS-I/II/III is presented. We confirm that: (1) the moderate anti-correlation between the fractional variations of Si IV BALs and the continuum in 74 quasars that show Phenomenon I; (2) the sample showing BAL variations tends to have larger ionizing continuum variations. These results reveal the ubiquitous effect of the continuum variability on Phenomenon I and BAL variation. We attribute the relative lack of variation of C IV BALs in Phenomenon I to the saturation effects. Nonetheless, these absorbers are not very optically thick in Si IV and the ionization changes in response to continuum variations could be the main driver of their variations. Finally, we find that the saturation effect on BAL variability can well explain many phenomena of BAL variations that have been reported before.

Keywords: galaxies: active — quasars: absorption lines

1. INTRODUCTION

At present, it is clear that both transverse motion (TM) and ionization change (IC) of outflow cloud can be mechanism that drives the variability of broad absorption line (BAL). Both these two sources of variability have observational evidences. For the TM scenario, early works have not found obvious relation between BAL and the continuum variability (Gibson et al. 2008; Wildy et al. 2014; Vivek et al. 2014); in recent works, the strength of P v in BAL outflows inferred that the BALs are very saturated with large total column densities, which may offer an evidence for the TM model (Moravec et al. 2017; Capellupo et al. 2017; McGraw et al. 2018). For the IC scenario, coordinated multi-trough variability (e.g., Capellupo et al. 2012, 2013; Filiz Ak et al. 2013; Wildy et al. 2014; Wang et al. 2015) and the coordinated variability between BALs and the ionizing continuum (Wang et al. 2015) have been found, these results tend to support the IC scenario. For instance, Filiz Ak et al. (2013) estimated that $(56 \pm 7)\%$ of trough variations are arising from a mechanism correlated between troughs, such as ionization changes. Besides, Wang et al. (2015) showed that BAL gas can in principle

show large changes in response to only small continuum variations. More recently, based on the multi-epoch observed BAL quasars from SDSS-I/II/III, He et al. (2017) have estimated statistically that at least 80% of the BAL variations are mainly driven by variations of the ionizing continuum. Based on the same data sample of He et al. (2017), Lu et al. (2018, hereafter LLQ2018) have revealed the moderate anti-correlations with a high significance level between fractional equivalent width (EW) variations ($\Delta EW / \langle EW \rangle$) of BALs (for both Si IV and C IV BALs) and the fractional flux variations of the continuum ($\Delta F_{\text{cont}} / \langle F_{\text{cont}} \rangle$).

Previous studies have found that BALs are frequently saturated but not black, which suggests that these absorbers do not completely obscure the continuum emitter (e.g., Hamann 1998; Arav et al. 1999b). Saturation of BALs has crucial influence on the exploration of BAL variability, because the EW measurements of saturated BALs can not accurately reflect the true value of optical depths and column densities (e.g., Hamann 1998; Arav et al. 1999b; Gabel et al. 2003). BALs do vary from days to years (e.g., Filiz Ak et al. 2013; Grier et al. 2015), but they can only weakly respond to the fluctu-

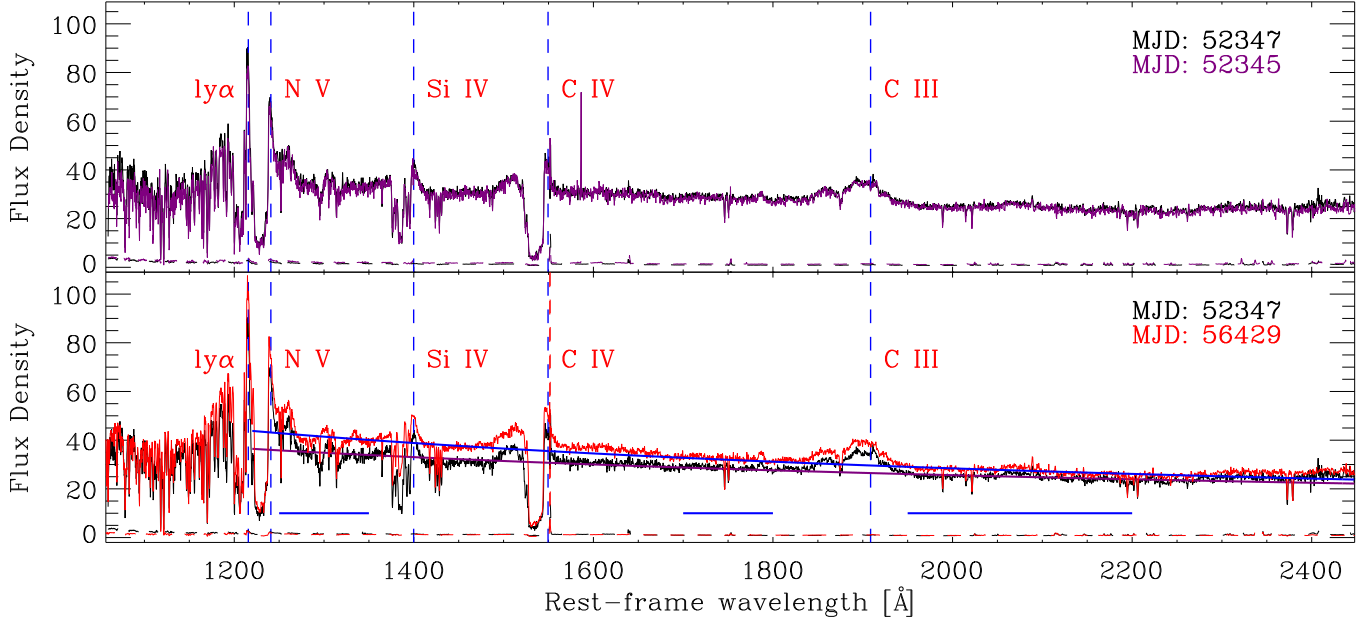


Figure 1. Three spectra of J1537+5829. The SDSS MJDs of the spectra are labeled. The flux density is in units of $10^{-17} \text{ erg s}^{-1} \text{ cm}^{-2}$. The dashed lines shown near the bottom of each panel are the formal 1σ errors. The blue vertical dashed lines mark out the main emission lines. The blue and purple lines in the bottom panel are the power-law continuum for spectra of J1537+5829 on MJD 52347 and 56429. The blue horizontal bars below the spectra are the regions used to fit the power-law continua.

ations of the ionizing continuum when the BAL troughs are highly saturated. Namely, a severely saturated C IV BAL will disfavour the IC scenario as the cause of its variability. If a severely saturated BAL still show time variation, then it tends to support the TM scenario as its variability cause. Thus, aiming to confirm the cause of BAL variability, some authors have attempted to prove the saturation of BAL systems (e.g., Arav et al. 1999a) at first by, for example, the detection of P V $\lambda\lambda 1118, 1128$ BALs (e.g., Hamann 1998; Capellupo et al. 2014, 2017; Moravec et al. 2017).

Since the BALs are frequently suffering from saturation, how do the saturation feature affect the BAL variation? What is the physical mechanism behind the variation of BAL that shows saturation feature? In this paper, we study a variation phenomenon that shows significant variation in Si IV BAL but no or only small change in C IV BAL (hereafter Phenomenon I). This interesting signature of BAL variation may offer clues to the above questions. We first give an analysis of a typical case showing Phenomenon I, quasar SDSS J153715.74+582933.9 ($z_{\text{em}} = 2.595$; Pâris et al. 2017; hereafter J1537+5829). And then we present a statistical study about the main driver of the variations of the BALs that show Phenomenon I, based on quasars multi-observed by SDSS-I/II/III. The paper is structured as follows. Section 2

presents the study of J1537+5829. Section 3 contains the details of the statistical analysis. Section 4 discusses the implications of saturation effect, and conclusions are provided in section 5.

2. A TYPICAL CASE SHOWING PHENOMENON I

Currently, Lu & Lin (2018, hereafter LL2018) have discovered that some of the BALs (Type N BALs¹) are actually a complex of NALs, and that the decomposition of a Type N BAL into NALs can serve as an effective way to study the BAL outflows. In this section, we present the analysis of a Type N BAL quasar J1537+5829, which shows Phenomenon I.

2.1. Spectroscopic analysis

J1537+5829 was observed by the Sloan Digital Sky Survey (SDSS; York et al. 2000) on MJD 52345 and 52347, and by the Baryon Oscillation Spectroscopic Survey (hereafter “BOSS”; Dawson et al. 2013) on MJD 56429. The SDSS spectra cover a wavelength range between ~ 3800 and 9200 \AA and have a resolution ranging from ~ 1850 to 2200 , while the BOSS spectrum covers

¹ This type of BALs was called as “Type II BALs” in LL2018. To avoid the potential for confusion “Type II BAL quasar” with narrow-line AGN which exhibit BAL troughs, we change the term to “Type N BALs” in this paper. Similarly, we rename the “Type I BALs”, which show relatively smooth BAL troughs that cannot be decomposed into multiple NALs, as “Type S BALs”.

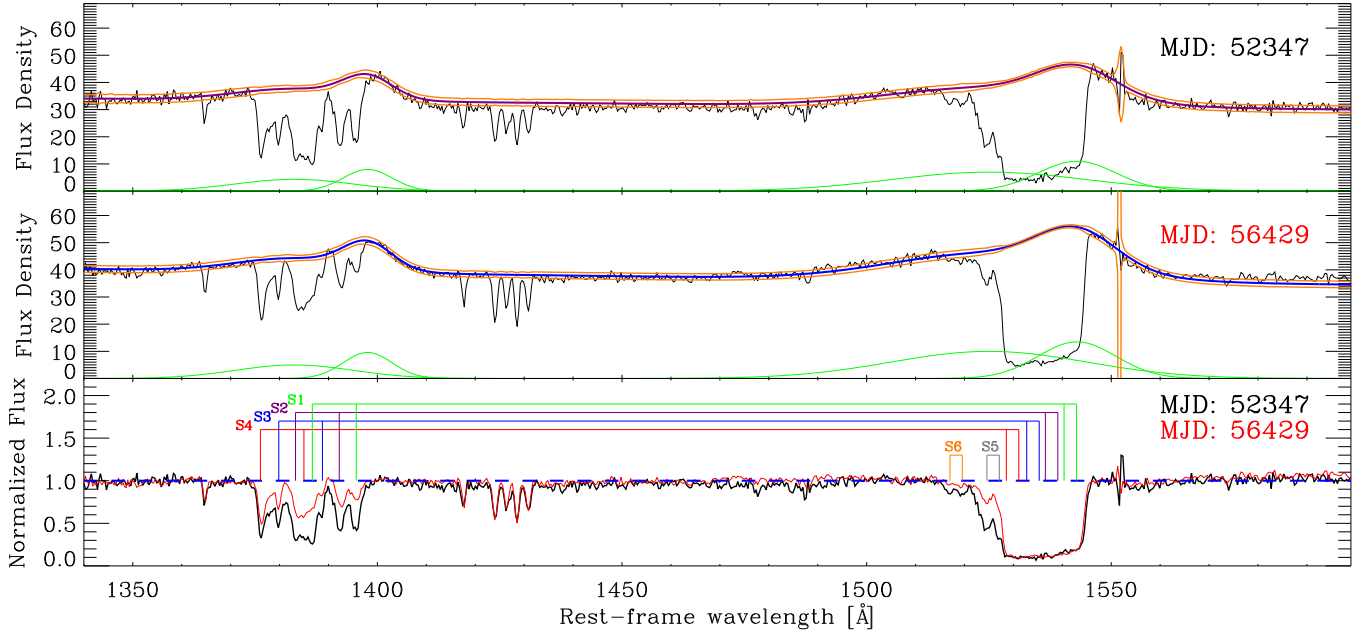


Figure 2. Pseudo-continuum fits (top and middle panels) and pseudo-continuum normalized spectra (bottom panel) of J1537+5829 on MJD 52347 and 56429. The flux density is in units of 10^{-17} erg s $^{-1}$ cm $^{-2}$. The purple line in the top panel and the blue line in middle panel are the pseudo-continua, the orange lines are the pseudo-continua that have added the flux uncertainties. The green Gaussian profiles in the bottom of the top and middle panels are the Gaussian components used to fit the Si IV and C IV emission lines. The green, purple, blue, red, grey and orange lines in the bottom panel mark out the six identified NAL systems within the Si IV and C IV BALs.

a wavelength from ~ 3600 to $10\,000$ Å and has a resolution within ~ 1300 to 3000 . The median signal-to-noise ratio (S/N) of the MJD 52345, 52347 and 56429 spectra of J1537+5829 are 16.75, 23.73 and 30.81 per pixel, respectively. In this section, we choose the last two spectra to study because: (1) the time interval between the first two observations is just 2 days, so that these two spectra are almost the same (Figure 1); (2) the last two spectra have higher S/N than the first one.

As a BAL quasar, J1537+5829 has been studied in some systematic BAL studies (Trump et al. 2006; Scaringi et al. 2009; Gibson et al. 2009; Allen et al. 2011; Bruni et al. 2014; Filiz Ak et al. 2014; He et al. 2015, 2017). The MJD 52347 spectrum of J1537+5829 has the balnicity index (BI; see the definition in Weymann et al. 1991) of 455.2 and 429.2 km s $^{-1}$ for the Si IV and C IV BALs (these estimations are taken from Allen et al. 2011), respectively. As Type N BALs, both the Si IV and C IV BALs in J1537+5829 actually contain multiple NAL systems, but they show different trough profiles: Si IV BAL shows multiple-absorption troughs, while the C IV BAL has a P-Cygni/trough-like shape.

Since the improved flux calibration of the SDSS data release 14 (DR14; Abolfathi et al. 2018), we downloaded the spectra of J1537+5829 from SDSS DR14. We then

fitted iteratively the power-law continuum for each spectrum based on several relatively line-free (RLF) wavelength regions (1250–1350, 1700–1800, 1950–2200, 2650–2710 Å in the rest frame; defined by Gibson et al. 2009). In order to reduce the influences of emission/absorption lines and/or remaining sky pixels, we removed the pixels that are outside 3σ significance during the fitting. The power-law continuum fits of the spectra are shown in Figure 1.

Figure 1 shows that both the Si IV and C IV BALs in J1537+5829 are superimposed on the corresponding emission lines. To measure the absorption lines more accurately, we fit the Si IV and C IV emission lines using Gaussian profiles. For the Si IV emission line, it fits well with two Gaussian components with full widths at half maximum (FWHMs) of 2525 and 6125 km s $^{-1}$ and velocity offsets of 386 and 3620 km s $^{-1}$, respectively. For the C IV emission line, it fits well with two Gaussian components with FWHMs of 3660 and 9258 km s $^{-1}$ and velocity offsets of 1256 and 4774 km s $^{-1}$, respectively. Combining the power-law continuum and the Gaussian profiles for emission lines, we got the final pseudo continuum for each spectrum (Figure 2). Then we measured the absorption lines in the pseudo-continuum normalized spectra.

Following LL2018, we did the additive fit to the com-

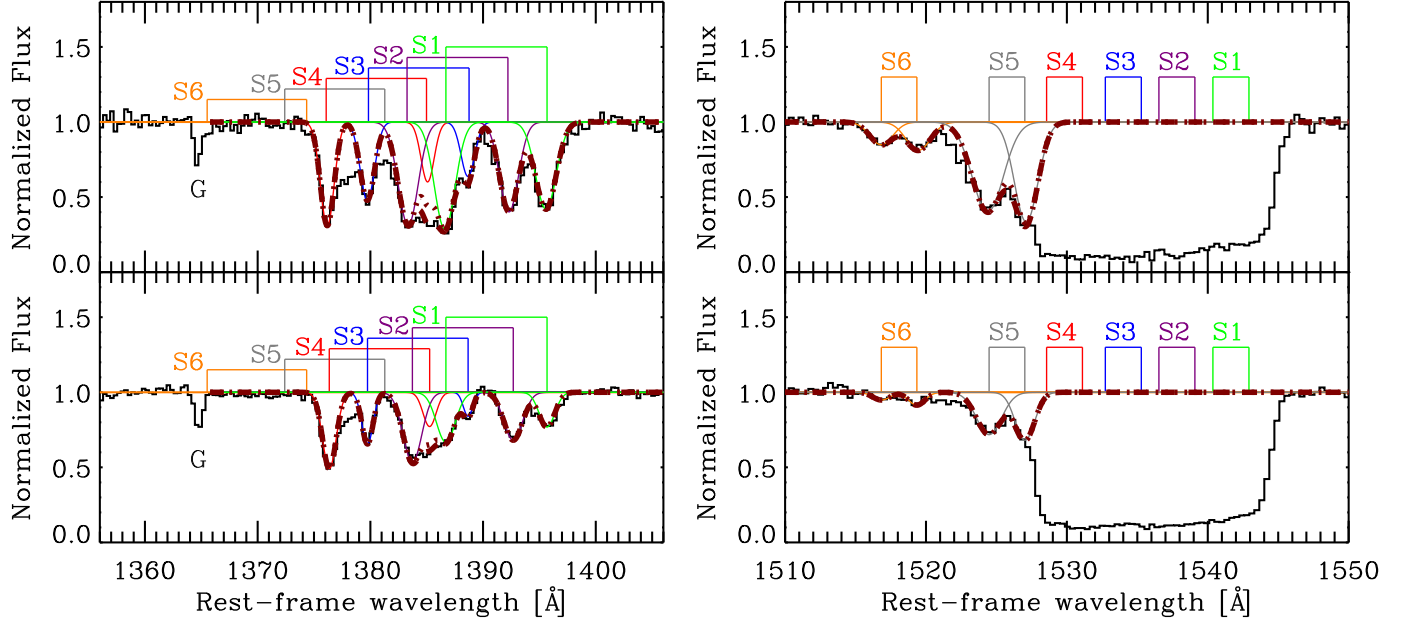


Figure 3. NAL absorption systems within the BALs in J1537+5829 (left panel: four NAL absorption systems (S1~S4) within the Si IV BAL trough; right panel: two NAL absorption systems (S5 and S6) within the C IV BAL trough). The top and bottom spectra are snippets from the MJD 52347 and 56429 normalized spectra, respectively. The brown broken lines and brown dotted lines represent the additive fit and multiplicative fit models, respectively. “G” marks a strong Galactics absorption line.

plex NALs within the Si IV BAL trough using four pairs of Gaussian functions (left panel of Figure 3). We also overplotted the spectrum resulting from multiplying together the residual fluxes from the additive fit as brown dotted lines. We demonstrate that the difference between the additive spectrum and the multiplicative spectrum is small in most of the wavelengths. But we note that the red component of S4 on MJD 52347 spectrum may suffer from a little underestimation according to the multiplicative spectrum. We also note that we can only identify the lower limit of the numbers of the absorption systems due to the low resolution of the SDSS/BOSS spectra and the blending of the absorption lines. For instance, there is absorption between the blue components of S3 and S4 in both epoches, which means that four Gaussian NALs are not sufficient to match the full Si IV BAL in this object. One may infer partial covering of the outflow from the “nonblack saturation” of C IV BALs. However, the low resolution of the SDSS/BOSS spectra also do not allow us to measure correctly the coverage fraction of NALs, we therefore accepted a full coverage during our line fitting. Although suffering from severe blending, two C IV NAL doublets at relatively higher outflow velocities can still be identified (the right panel of Figure 3).

We measured the velocity, EW, FWHM and fractional EW variation of the absorption lines based on the Gaus-

sian fits. The methods for calculating the EWs of absorption line are the same to LL2018 (see Equations (1), (2) and (3) of LL2018), for calculating the fractional EW variations are the same to LLQ2018 (Equation (2) of LLQ2018). Measurements of the absorption lines are listed in Table 1.

2.2. Evidence for IC

We hold the view that the mechanism responsible for the absorption-line variability in J1537+5829 is the IC scenario for two reasons: (1) coordinated multiple-trough weakening; (2) obvious continuum strengthening. For the first reason, well coordinated variations between multiple NAL/BAL systems (e.g., Hamann et al. 2011; Chen & Qin 2015; Wang et al. 2015; McGraw et al. 2017) or over a large velocity interval of a BAL trough (e.g., Grier et al. 2015; McGraw et al. 2017, 2018) can serve as strong evidence supporting the IC scenario to explain absorption variation. Phenomenon of coordinated absorption-line variability is difficult to be explained by the TM scenario because it would require coordinated motions of many distinct outflow structures (Misawa et al. 2005; Hamann et al. 2011). In the case of J1537+5829, the coordinated weakening among different NAL absorption systems (S1~S4) within the Si IV BAL trough is detected (see Figure 2, Figure 3 and Table 1). Although belonging to the same systems with the Si IV

Table 1. Measurements of Si IV and C IV BALs

Species	z_{abs}	Velocity (km s ⁻¹)	MJD:52347		MJD:56429		Fractional EW variation	Note
			EW (Å)	FWHM (km s ⁻¹)	EW (Å)	FWHM (km s ⁻¹)		
Si IV λ 1393	2.5497	3805	1.07 ± 0.03	314	0.79 ± 0.03	314	-0.15 ± 0.046	S4
Si IV λ 1402			0.59 ± 0.04	298	0.34 ± 0.06	298	-0.27 ± 0.062	
Si IV λ 1393	2.5588	3031	0.84 ± 0.04	327	0.44 ± 0.04	256	-0.31 ± 0.052	S3
Si IV λ 1402			0.56 ± 0.05	311	0.17 ± 0.07	212	-0.53 ± 0.064	
Si IV λ 1393	2.5682	2246	1.54 ± 0.03	454	0.98 ± 0.04	426	-0.22 ± 0.038	S2
Si IV λ 1402			1.26 ± 0.04	423	0.67 ± 0.06	423	-0.31 ± 0.042	
Si IV λ 1393	2.5766	1542	1.65 ± 0.03	467	0.7 ± 0.05	425	-0.40 ± 0.037	S1
Si IV λ 1402			1.34 ± 0.04	464	0.41 ± 0.07	352	-0.53 ± 0.041	
C IV λ 1548	2.5222	6136	0.31 ± 0.18	378	0.08 ± 0.64	285	-0.59 ± 0.084	S6
C IV λ 1551			0.42 ± 0.17	401	0.13 ± 0.56	271	-0.53 ± 0.073	
C IV λ 1548	2.5397	4647	1.70 ± 0.04	515	0.34 ± 0.07	412	-0.67 ± 0.036	S5
C IV λ 1551			1.41 ± 0.03	386	0.21 ± 0.05	322	-0.74 ± 0.040	
C IV BAL	...	$-4283 \sim -674^{\text{a}}$	14.94 ± 1.22	3609^{b}	14.62 ± 0.62	3609^{b}	-0.01 ± 0.007	S1~S4
C IV BAL	...	$-6785 \sim -674^{\text{a}}$	18.55 ± 1.77	6111^{b}	16.09 ± 0.95	6111^{b}	-0.07 ± 0.006	S1~S6
Si IV BAL	...	$-5576 \sim -279^{\text{a}}$	10.15 ± 1.73	5297^{b}	4.84 ± 0.95	5297^{b}	-0.35 ± 0.010	S1~S4

^aVelocity range of the BAL troughs with respect to emission rest frame.^bTotal width calculated from edge-to-edge of the BAL troughs.

NAL components, the S1~S4 NAL components within the C IV BAL trough show no obvious variation between the two observations. We ascribe this phenomenon to the saturation in C IV. As shown in Figure 2 and Table 1, the NAL components (S1~S4) of C IV show larger EWs than Si IV and are blended severely, resulting in a typical trough-like profile but not black. This suggests that these C IV NAL components (S1~S4) are saturated and do not completely obscure the emission regions at these wavelengths (continuum emission region and C IV broad emission line region). However, the other two absorption systems (S5 and S6) within the C IV BAL, which are relatively weaker at higher outflow velocities, do show coordinated weakening. Thus we speculate that the coordinated ionization state variations have occurred in the saturated NAL components (S1~S4) within the C IV BAL.

For the second reason, anti-correlations between the variations of the ionizing continuum and UV outflow lines have been proved recently (Lu et al. 2017; LLQ2018), which can serve as evidence for the idea: the IC scenario is the primary driver of UV absorption-trough variability. Thus, the continuum variation can reveal the cause of UV absorption line variability, to some extent. In the case of J1537+5829, while the absorption lines show coordinated weakening between the two observations, the power-law continuum shows a fractional enhancing of 0.12 ± 0.025 (see also Figure 1). This is compatible with the previous anti-correlation. Based on the above analysis, we ascribe the absorption-line variability in J1537+5829 to the IC scenario, which is the respond to the variation of the ionizing continuum.

Based on the case of J1537+5829, we point out that the saturation signature of a C IV BAL does not always mean that the TM scenario is the driver of the variation of this BAL system. Although most areas in the saturated C IV BAL in J1537+5829 lack variability, the coordinated ionization variations of the outflow structures are confirmed due to the coordinated variation of Si IV NALs at the corresponding velocities.

2.3. Comparison with LL2018

As another case of showing Type N BALs, J1537+5829 has many similar qualities compared to the quasar example, J002710.06–094435.3 (hereafter J0027–0944), in LL2018. First and foremost, both the Si IV and C IV BALs consist of multiple NAL components that show coordinated time variations for both these two quasars. In fact, the discussions for J0027–0944 in LL2018, on the origin and variability cause of the BALs (section 3.1 of LL2018), the constraints on the inclination model (section 3.2 of LL2018), the explanation for different profile shapes of BALs (section 3.3 of LL2018) and the clumpy structure of outflows (section 3.4 of LL2018), all apply

equally to J1537+5829. The biggest difference between these two sources is that the C IV BAL shows global variation in J0027–0944 while only small partial change in J1537+5829. However, we do not think that these two C IV BALs are fundamentally different. The essential reason for this difference is that the C IV BAL of J1537+5829 suffers from more saturation than that of J0027–0944. Through the cases of J1537+5829 and J0027–0944, we find that the decomposition of a BAL into NALs can serve as an effective way to determine the mechanism of absorption-line variability. In fact, the essence of the global variation of a Type N BAL is the coordinated variability of multiple NALs.

The phenomenon of the NAL complex as a form of BALs reveals that the line of sight intersects several physically separated outflow components. If the Type N BALs is universal, then it may serve as evidence that the outflow is clumpy in physical space, which, to some extent, supports the schematic of inhomogeneous partial coverage (IPC; Hamann et al. 2001; de Kool et al. 2002; Hamann & Sabra 2004; Arav et al. 2005; Sabra & Hamann 2005). More significantly, recent numerical simulations by Matthews et al. (2016) show that the ionization state can be moderated sufficiently at more realistic X-ray luminosities when incorporating clumping with a filling factor of ~ 0.01 . Namely, clumpy structure of outflow may be self-shielded and thus may offer another explanation to solve the overionization problem (see also Hamann et al. 2013). Later systematic study on Type N BALs will quantitatively determine the universality of Type N BALs in outflows (Lu et al., in preparation), which may provide more insights into the above discussion.

3. STATISTICAL ANALYSIS

To investigate the main driver of the BAL variations in cases like J1537+5829 showing Phenomenon I, we present a statistical analysis based on the BAL sample selected from SDSS-I/II/III.

3.1. Sample selection

Our multi-observed BAL sample was derived from the catalog provided by He et al. (2017). This catalog contains 9918 spectrum pairs in 2005 BAL quasars (hereafter the Total sample) with a redshift range of $1.9 < z < 4.7$ and a signal-to-noise ratio (S/N) level of $S/N > 10$ in at least one observation. First of all, we downloaded these spectra from SDSS DR14 and fitted the power-law continuum for each of them using the same procedure described in LLQ2018. The strength of the ionizing continuum of each spectrum was estimated using the power-law continuum flux at 1450 Å. Then we only keep quasars that meet two criteria: (1) the Si IV BAL shows significant

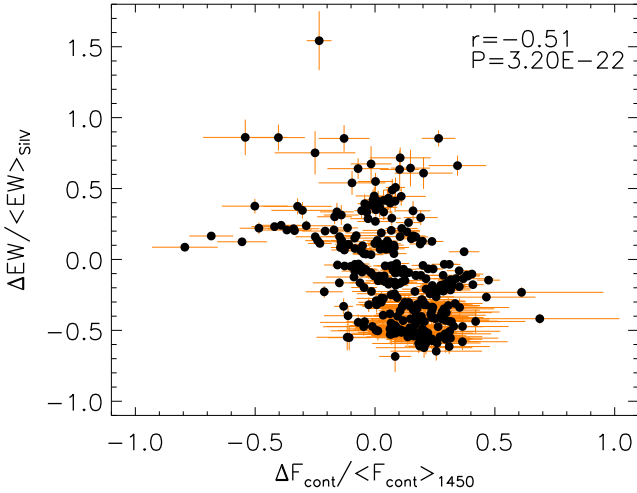


Figure 4. Plots of fractional EW variations of Si IV BALs and fractional flux variations of the continuum. The median error values of $\Delta EW/\langle EW \rangle_{\text{SiIV}}$ and $\Delta F_{\text{cont}}/\langle F_{\text{cont}} \rangle_{1450}$ are 0.040 and 0.082, respectively.

variation (with a confident level of $\Delta W > 5\sigma^2$); (2) the absolute value of fractional EW variation of C IV BAL less than 0.08 (this threshold is chosen referring to the fractional C IV BAL variation in J1537+5829). Finally, including J1537+5829, we found 318 spectrum pairs in 74 quasars (hereafter the Phenomenon I sample) meet these criteria.

3.2. Correlation between fractional variations of Si IV BALs and the continuum

We plotted the fractional variation of Si IV BALs ($\Delta EW/\langle EW \rangle_{\text{SiIV}}$) versus the fractional variation of the continuum ($\Delta F_{\text{cont}}/\langle F_{\text{cont}} \rangle_{1450}$) in Figure 4. The moderate anti-correlation between them was confirmed by the Spearman rank correlation analysis ($r = -0.51$, $P = 3.20\text{E} - 22$). This anti-correlation is an important finding to understand the variation mechanism on Phenomenon I. In fact, Phenomenon I has been mentioned in previous works (e.g., Misawa et al. 2014; Wang et al. 2015; McGraw et al. 2018). Misawa et al. (2014) and McGraw et al. (2018) held the view that the IC scenario was the most plausible explanation for Phenomenon I. Wang et al. (2015) pointed out that there may not be a physical difference between the variable and non-variable portions of a absorption trough, because there may exist some absorption variations that we cannot detect, even for those caused by moderate variability in the ion column density. However, in previous work, there has been no convincing evidence to demonstrate the main driver of Phenomenon I, because no one has studied the behavior of cases where Si IV absorption varies but C IV absorption

does not. Importantly, our statistical results provide evidence for the ubiquitous effect of the ionizing continuum variability on the Phenomenon I.

We attribute the relative lack of variation of the C IV BALs to the saturation effect. Nonetheless, moderate anti-correlation exists between the fractional variations of the ionizing continuum and Si IV BALs, indicating that most of the absorbers are not very optically thick in Si IV since a highly saturated trough should not show fractional EW variations in response to ionizing continuum variability. The range of variation seen for Si IV in Figure 4 is consistent with that seen by Filiz Ak et al. 2014 (their Figure 14), when the fractional C IV EW variation limit is considered.

Before this paper, anti-correlation between the fractional flux variations of the continuum and fractional EW variations of both C IV and Si IV BALs has been confirmed for a quasar sample (1014 spectrum pairs in 483 quasars, hereafter the LLQ2018 sample) that shows significant variations for both C IV and Si IV BALs (LLQ2018). Phenomenon I sample is the expansion and extension of the LLQ2018 sample, and the anti-correlations presented in these two papers have the consistency in essence. The difference between these two samples is that the BALs in the Phenomenon I sample suffer from more saturations in C IV than that in the LLQ2018 sample.

In summary, the correlation between fractional variations of Si IV BALs and the continuum for the Phenomenon I sample confirms that these BALs are indeed suffering from saturations in C IV, but the IC scenario is still a main driver for their variations in Si IV.

3.3. Distributions of fractional variations of Si IV BALs and the continuum

It is shown in Figure 4 that most of the data points have a positive $\Delta F_{\text{cont}}/\langle F_{\text{cont}} \rangle_{1450}$ value but a negative $\Delta EW/\langle EW \rangle_{\text{SiIV}}$ value. To investigate the cause of this phenomenon, we plotted $\Delta F_{\text{cont}}/\langle F_{\text{cont}} \rangle_{1450}$ and $\Delta EW/\langle EW \rangle_{\text{SiIV}}$ distributions for the Total sample, the LLQ2018 sample and the Phenomenon I sample (Figure 5), respectively. KS tests show that the $\Delta F_{\text{cont}}/\langle F_{\text{cont}} \rangle_{1450}$ and $\Delta EW/\langle EW \rangle_{\text{SiIV}}$ distributions for the three samples are significantly ($P < 1\text{E} - 8$) different from each other.

Although the $\Delta F_{\text{cont}}/\langle F_{\text{cont}} \rangle_{1450}$ distributions show no obvious deviation from symmetry about zero for both the Total sample (with the center $\mu = 0.017$ for the best-fitting Gaussian component) and the LLQ2018 sample (with the center $\mu = 0.029$ for the best-fitting Gaussian component), the absolute values of $\Delta F_{\text{cont}}/\langle F_{\text{cont}} \rangle_{1450}$ for the LLQ2018 sample (with the standard deviation $\sigma = 0.265$ for the best-fitting Gaussian component) tend to be larger than that for the Total sample (with the

² See Equation (1) of LLQ2018 for the definition of ΔW .

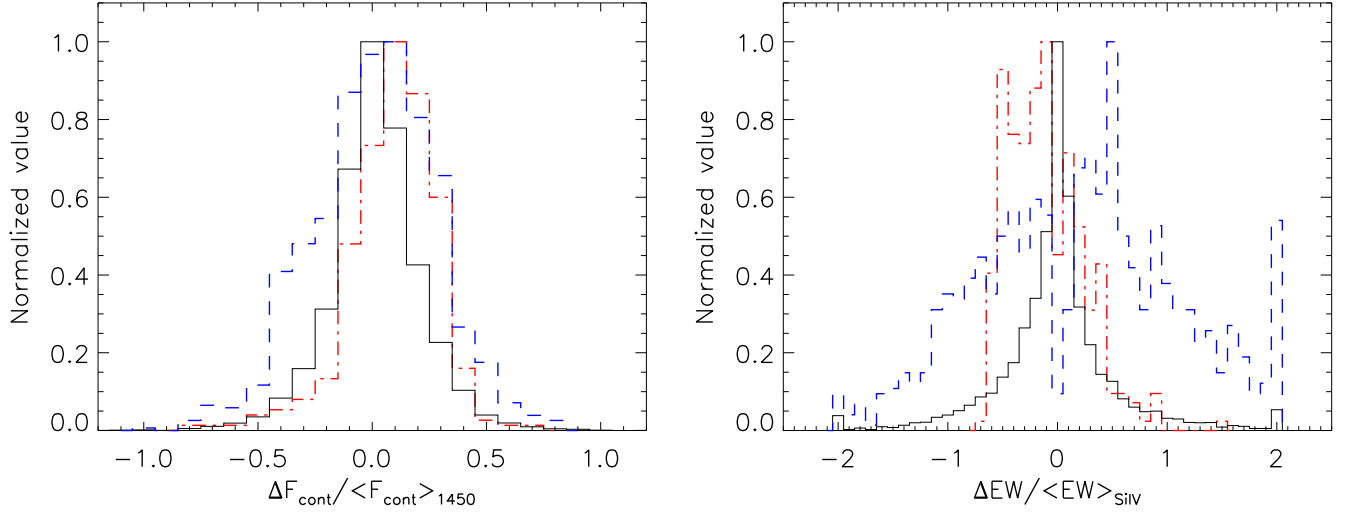


Figure 5. $\Delta F_{\text{cont}}/\langle F_{\text{cont}} \rangle_{1450}$ (left panel) and $\Delta \text{EW}/\langle \text{EW} \rangle_{\text{SiIV}}$ (right panel) distributions for the Total sample (solid black), the LLQ2018 sample (dashed blue) and the Phenomenon I sample (dot-dashed red). Each histogram is normalized to their corresponding maximum value. KS test results indicate that the distributions of $\Delta F_{\text{cont}}/\langle F_{\text{cont}} \rangle_{1450}$ and $\Delta \text{EW}/\langle \text{EW} \rangle_{\text{SiIV}}$ show significant ($P < 1\text{E} - 8$) differences between the three samples.

standard deviation $\sigma = 0.156$ for the best-fitting Gaussian component). This indicates that the sample showing BAL variations tends to have larger ionizing continuum variations. Such phenomenon is reasonable when considering that change of the ionizing continuum as the primary driver of BAL variability (Wang et al. 2015; He et al. 2017; LLQ2018).

The distributions of $\Delta F_{\text{cont}}/\langle F_{\text{cont}} \rangle_{1450}$ and $\Delta \text{EW}/\langle \text{EW} \rangle_{\text{SiIV}}$ for the Phenomenon I sample show deviations from symmetry about zero in opposite direction (with the center $\mu = 0.116$ and $\mu = -0.185$ of the Gaussian for $\Delta F_{\text{cont}}/\langle F_{\text{cont}} \rangle_{1450}$ and $\Delta \text{EW}/\langle \text{EW} \rangle_{\text{SiIV}}$ distributions, respectively). We attribute this trend to the saturation effect on the photoionization-driven BAL variability. An important feature of the Phenomenon I sample is that their CIV BALs are generally suffering from saturations. This feature is also reflected in the $\Delta \text{EW}/\langle \text{EW} \rangle_{\text{SiIV}}$ distribution. Because the fractional EW variation measurements can reflect only the lower limits of the optical depth and column density variations for saturated troughs, the $\Delta \text{EW}/\langle \text{EW} \rangle_{\text{SiIV}}$ distribution of the Phenomenon I sample (with the standard deviation $\sigma = 0.362$ for the best-fitting Gaussian component) tends to have smaller absolute values than the LLQ2018 sample (with the standard deviation $\sigma = 1.042$ for the best-fitting Gaussian component). Since the anti-correlation between the fractional variations of BALs and the continuum has been built (LLQ2018; Section 3.2), the strengthening of BALs are expected when the ionizing continuum is weakening. However, on the one hand, the EW for a saturated BAL may unable to be enhanced when its ionization-level changes. On the

other hand, the strengthening of the ionizing continuum may weaken a saturated BAL if it is not very optically thick. Thus the distributions of the $\Delta F_{\text{cont}}/\langle F_{\text{cont}} \rangle_{1450}$ and $\Delta \text{EW}/\langle \text{EW} \rangle_{\text{SiIV}}$ of the Phenomenon I sample show deviations from symmetry about zero in opposite direction, which provides statistical evidence for two physical processes in some saturated BALs: (1) photoionization-driven transition from saturated to unsaturated; (2) recombination-driven column density strengthening with no significant EW variation.

4. IMPLICATIONS OF SATURATION EFFECT

4.1. Dispersion of the relations between fractional variations of the continuum and BALs

The effect of saturation on BALs can well interpret many phenomena of BAL variation that have been discovered previously. For example, LLQ2018 found that although correlations with high significance level are detected, relations between the fractional flux variations of the continuum and fractional EW variations for both SiIV and CIV BALs show large dispersion (hereafter Trend I). Such dispersion is also confirmed in the Phenomenon I sample (see Figure 4). We attribute partly this dispersion to the effect of BAL saturation, because the measurements of the fractional EW variation can not accurately reflect the fractional variations of the optical depth and column density for saturated troughs, they reflect only their lower limits (Arav et al. 1999b, 2005). As in the case of J1537+5829, the EW of the CIV BAL show no obviously variation due to the effect of saturation, so the fractional EW variation of CIV BAL trough can not reflect the true values of the fractional variation

of optical depth and column density.

4.2. Larger fractional EW variations for Si IV than C IV BALs

Previous works have found that Si IV BALs generally show larger fractional EW variations than C IV BALs (hereafter Trend II e.g., [Filiz Ak et al. 2013](#), [LLQ2018](#)). Just as [LLQ2018](#) pointed out, Trend II can attribute to the different fundamental parameters from atomic physics, typically fine structure and oscillator strength, between Si IV and C IV (see also section 3.3 of [LL2018](#) for detail description). In fact, the Phenomenon I is the extreme of Trend II, rather than a qualitatively distinct phenomenon. The universality of Trend II also reveals the universality of the saturation in BALs. Based on the above explanations of Trend II, we find that the EW measurements of Si IV BAL are statistically more accurate than C IV BAL when reflecting the true values of optical depth and column density. So it is not hard to understand why the correlation coefficient between the fractional flux variations of the continuum and fractional EW variations of Si IV are larger than that of C IV (table 1 in [LLQ2018](#)). As in J1537+5829, a typical case showing Trend II, the Si IV BAL shows a fractional EW variation of -0.35 ± 0.010 , while the C IV BAL shows a fractional EW variation of only -0.07 ± 0.006 (see Table 1).

4.3. Larger fractional EW variations in weaker BAL troughs

Previous studies have found that Si IV and C IV BAL variations usually occur in relatively weak troughs, and that weak troughs tend to have larger fractional EW variations than strong troughs (hereafter Trend III; e.g., [Lundgren et al. 2007](#); [Gibson et al. 2008](#); [Capellupo et al. 2011](#); [Filiz Ak et al. 2013](#); [McGraw et al. 2018](#)). Trend III is understandable if weaker absorption troughs are less saturated. If the weaker absorption troughs tend to suffer less saturation than the stronger ones, then the weaker ones would show more variations when responding to the same changes in ionization condition. Of course, previous studies also found that the absorption troughs in high velocity tend to be weaker and more variable (e.g., [Gibson et al. 2009](#); [Capellupo et al. 2011](#); [Filiz Ak et al. 2012, 2013](#)). Those weaker troughs in higher outflow velocity may have a different origin from the stronger troughs in lower outflow velocity, thus Trend III may be caused by a velocity effect. However, [Filiz Ak et al. \(2013\)](#) demonstrated that the trough weakness rather than a velocity effect is the main driver of Trend III, by taking the Spearman test on the fractional EW variation versus both average EW over the two relevant epochs and outflow velocity of C IV BALs in 291 quasars (see fig.18

of [Filiz Ak et al. 2013](#)). Thus, Trend III may attribute mostly to the saturation effect.

4.4. BAL trough often shows only partial variations

Previous studies have showed that variability often occurs only in a portion of a BAL trough (hereafter Trend IV; e.g., [Gibson et al. 2008](#); [Capellupo et al. 2011, 2012, 2013](#); [Filiz Ak et al. 2013](#)). Some authors tend to believe that Trend IV fits the TM scenario more naturally than the IC scenario (e.g., [Capellupo et al. 2012, 2013](#)). We do not rule out the possibility that the TM scenario may account for Trend IV. However, we point out that saturation effect on photoionization-driven Type N BAL variability is also easy to generate Trend IV. From the point of view of Type N BAL, a BAL shows saturation feature in large portions dose not mean that all NAL systems inside this BAL are saturated. Just like the case of J1537+5829, though the saturated NAL components (S1~S4) inside C IV BAL are blended severely resulting in a typical trough-like profile, the other two weaker and relatively-high-speed NAL components (S5 and S6) inside the same trough still show time variations, which can be explained by IC scenario. Also, the undetectable EW variation of the saturated NAL components (S1~S4) dose not mean the unchange in their ionization level and column density. Based on the above discussions, we argue that Trend IV does not always mean the TM scenario as the driver of the variability, instead, the IC scenario can also responsible for Trend IV.

5. CONCLUSION

We have defined Phenomenon I, which shows significant variation in Si IV BAL but no or only small change in C IV BAL. The study of this interesting phenomenon help us understand the role of the saturation feature plays in BAL variation and the physical mechanism behind the variation of saturated BAL. We have shown a typical case of Type N BAL quasar showing Phenomenon I and have presented a statistical analysis based on multi-observed quasars from SDSS-I/II/III. Below we summarize our works.

1. Based on the two-epoch spectra of J1537+5829, we successfully identify four NAL systems (S1~S4) within its Si IV BAL and two additional NAL systems (S5 and S6) within its C IV BAL. The coordinated weakening of all of these NAL systems and the obvious strengthening of the quasar continuum collectively provide evidence supporting the ionization changes in response to the continuum variations to explain the BAL variability in J1537+5829. We ascribe the none variation of the S1~S4 NAL systems in the C IV BAL trough to their saturation. See Section 2.

2. Our statistical analysis based on 74 multi-observed quasars showing Phenomenon I confirms the moderate anti-correlation between the fractional variations of SiIV BALs and the continuum, revealing the ubiquitous effect of the ionizing continuum variability on Phenomenon I. Note that in Phenomenon I, the CIV BAL is strongly saturated but the SiIV BAL is not. We attribute the relative lack of variation of CIV BALs in Phenomenon I to the saturation effects. Besides, the above moderate anti-correlation indicates that these absorbers are not very optically thick in SiIV, and the ionization changes in response to the continuum variations is still the main driver of their variations. See Section 3.2.
3. The absolute values of $F_{\text{cont}}/\langle F_{\text{cont}} \rangle_{1450}$ for the LLQ2018 sample tend to be larger than that for the Total sample. This indicates that the sample showing BAL variations tends to have larger ionizing continuum variations, which serve as a clear result in support of the ionizing continuum variations being responsible for many BAL variations. See Section 3.3.
4. The $F_{\text{cont}}/\langle F_{\text{cont}} \rangle_{1450}$ and $\Delta\text{EW}/\langle \text{EW} \rangle_{\text{SiIV}}$ distributions for the Phenomenon I sample show deviations from symmetry about zero in opposite direction. This can be explained by the saturation effect on the photoionization-driven BAL variability. See Section 3.3.
5. Finally, we demonstrate that the saturation effect on BAL variability can well explain many phenomena of BAL variations that have been reported before. See Section 4.

We are very grateful to the anonymous referee for a lot of comments, which greatly improved the quality of this article. In addition, we thank He et al. (2018) for making the multi-observed BAL catalog publicly available.

Funding for SDSS-III was provided by the Alfred P. Sloan Foundation, the Participating Institutions, the National Science Foundation, and the US Department of Energy Office of Science. The SDSS-III web site is <http://www.sdss3.org/>.

SDSS-III is managed by the Astrophysical Research Consortium for the Participating Institutions of the SDSSIII Collaboration, including the University of Arizona, the Brazilian Participation Group, Brookhaven National Laboratory, Carnegie Mellon University, University of Florida, the French Participation Group, the German Participation Group, Harvard University, the Instituto de Astrofísica de Canarias, the Michigan

State/Notre Dame/JINA Participation Group, Johns Hopkins University, Lawrence Berkeley National Laboratory, Max Planck Institute for Astrophysics, Max Planck Institute for Extraterrestrial Physics, New Mexico State University, New York University, OhioState University, Pennsylvania State University, University of Portsmouth, Princeton University, the Spanish Participation Group, University of Tokyo, University of Utah, Vanderbilt University, University of Virginia, University of Washington, and Yale University.

REFERENCES

- Abolfathi, B., Aguado, D. S., Aguilar, G., et al. 2018, *ApJS*, 235, 42
- Allen, J. T., Hewett, P. C., Maddox, N., Richards, G. T., & Belokurov, V. 2011, *VizieR Online Data Catalog*, 741
- Arav, N., Becker, R. H., Laurent-Muehleisen, S. A., et al. 1999a, *ApJ*, 524, 566
- Arav, N., Kaastra, J., Kriss, G. A., et al. 2005, *ApJ*, 620, 665
- Arav, N., Korista, K. T., de Kool, M., Junkkarinen, V. T., & Begelman, M. C. 1999b, *ApJ*, 516, 27
- Bruni, G., González-Serrano, J. I., Pedani, M., et al. 2014, *A&A*, 569, A87
- Capellupo, D. M., Hamann, F., & Barlow, T. A. 2014, *MNRAS*, 444, 1893
- Capellupo, D. M., Hamann, F., Shields, J. C., Halpern, J. P., & Barlow, T. A. 2013, *MNRAS*, 429, 1872
- Capellupo, D. M., Hamann, F., Shields, J. C., Rodríguez Hidalgo, P., & Barlow, T. A. 2011, *MNRAS*, 413, 908
- . 2012, *MNRAS*, 422, 3249
- Capellupo, D. M., Hamann, F., Herbst, H., et al. 2017, *MNRAS*, 469, 323
- Chen, Z.-F., & Qin, Y.-P. 2015, *ApJ*, 799, 63
- Dawson, K. S., Schlegel, D. J., Ahn, C. P., et al. 2013, *AJ*, 145, 10
- de Kool, M., Korista, K. T., & Arav, N. 2002, *ApJ*, 580, 54
- Filiz Ak, N., Brandt, W. N., Hall, P. B., et al. 2012, *ApJ*, 757, 114
- . 2013, *ApJ*, 777, 168
- . 2014, *ApJ*, 791, 88
- Gabel, J. R., Crenshaw, D. M., Kraemer, S. B., et al. 2003, *ApJ*, 583, 178
- Gibson, R. R., Brandt, W. N., Schneider, D. P., & Gallagher, S. C. 2008, *ApJ*, 675, 985
- Gibson, R. R., Jiang, L., Brandt, W. N., et al. 2009, *ApJ*, 692, 758
- Grier, C. J., Hall, P. B., Brandt, W. N., et al. 2015, *ApJ*, 806, 111
- Hamann, F. 1998, *ApJ*, 500, 798
- Hamann, F., Chartas, G., McGraw, S., et al. 2013, *MNRAS*, 435, 133
- Hamann, F., & Sabra, B. 2004, in *Astronomical Society of the Pacific Conference Series*, Vol. 311, *AGN Physics with the Sloan Digital Sky Survey*, ed. G. T. Richards & P. B. Hall, 203
- Hamann, F. W., Barlow, T. A., Chaffee, F. C., Foltz, C. B., & Weymann, R. J. 2001, *ApJ*, 550, 142
- Hamann, J., Hannestad, S., Raffelt, G. G., & Wong, Y. Y. Y. 2011, *J. Cosmology Astropart. Phys.*, 9, 034
- He, Z., Wang, T., Zhou, H., et al. 2017, *ApJS*, 229, 22
- He, Z.-C., Bian, W.-H., Ge, X., & Jiang, X.-L. 2015, *MNRAS*, 454, 3962
- Lu, W.-J., & Lin, Y.-R. 2018, *MNRAS*, 474, 3397
- Lu, W.-J., Lin, Y.-R., & Qin, Y.-P. 2018, *MNRAS*, 473, L106
- Lu, W.-J., Lin, Y.-R., Qin, Y.-P., et al. 2017, *MNRAS*, 468, L6
- Lundgren, B. F., Wilhite, B. C., Brunner, R. J., et al. 2007, *ApJ*, 656, 73

- Matthews, J. H., Knigge, C., Long, K. S., et al. 2016, MNRAS, 458, 293
- McGraw, S. M., Shields, J. C., Hamann, F. W., Capellupo, D. M., & Herbst, H. 2018, MNRAS, 475, 585
- McGraw, S. M., Brandt, W. N., Grier, C. J., et al. 2017, MNRAS, 469, 3163
- Misawa, T., Charlton, J. C., & Eracleous, M. 2014, ApJ, 792, 77
- Misawa, T., Eracleous, M., Charlton, J. C., & Tajitsu, A. 2005, ApJ, 629, 115
- Moravec, E. A., Hamann, F., Capellupo, D. M., et al. 2017, MNRAS, 468, 4539
- Pâris, I., Petitjean, P., Ross, N. P., et al. 2017, A&A, 597, A79
- Sabra, B. M., & Hamann, F. 2005, ArXiv Astrophysics e-prints, astro-ph/0509421
- Scaringi, S., Cottis, C. E., Knigge, C., & Goad, M. R. 2009, MNRAS, 399, 2231
- Trump, J. R., Hall, P. B., Reichard, T. A., et al. 2006, ApJS, 165, 1
- Vivek, M., Srianand, R., Petitjean, P., et al. 2014, MNRAS, 440, 799
- Wang, T., Yang, C., Wang, H., & Ferland, G. 2015, ApJ, 814, 150
- Weymann, R. J., Morris, S. L., Foltz, C. B., & Hewett, P. C. 1991, ApJ, 373, 23
- Wildy, C., Goad, M. R., & Allen, J. T. 2014, MNRAS, 437, 1976
- York, D. G., Adelman, J., Anderson, Jr., J. E., et al. 2000, AJ, 120, 1579